Hindawi

Research Article

Synthesis, Characterization, and *In Vivo* Cytokinome Profile of IL-12-Loaded PLGA Nanospheres

Ryan A. Lacinski [iD],[1] **Justin E. Markel** [iD],[1] **Jabeen Noore,**[1] **Hillary G. Pratt** [iD],[2] **and Brock A. Lindsey** [iD][1]

[1]*Department of Orthopaedics, West Virginia University, Morgantown, WV, USA*
[2]*Department of Surgery, West Virginia University, Morgantown, WV, USA*

Correspondence should be addressed to Brock A. Lindsey; blindsey@hsc.wvu.edu

We report the successful encapsulation and elution of recombinant murine IL-12 (rmIL-12) from poly(lactide-co-glycolic) acid (PLGA) nanospheres (IL-12-NS) synthesized using the double emulsion/solvent evaporation (DESE) technique with microsphere depletion through ultracentrifugation. Images obtained with scanning electron microscopy (SEM) showcased a characteristic spherical shape with a mean particle diameter of 138.1 ± 10.8 nm and zeta potential of -15.1 ± 1.249 mV. These values suggest minimal flocculation when in solution, which was reflected in an *in vivo* biodistribution study that reported no observed morbidity/mortality. Encapsulation efficiency (EE) was determined to be $0.101 \pm 0.009\%$ with average particle concentration obtained per batch of $1.66 \times 10^9 \pm 4.45 \times 10^8$ particles/mL. Disparate zeta (ζ) potentials obtained from both protein-loaded and protein-unloaded batches suggested surface adsorption of protein, and confocal microscopy of BSA-FITC-loaded nanospheres confirmed the presence of protein within the polymeric shell. Furthermore, elution of rmIL-12 from IL-12-NS at a concentration of 500 million particles/mL was characterized using enzyme-linked immunosorbent assay (ELISA). When IL-12-NS was administered *in vivo* to female BALB/c mice through retroorbital injection, IL-12-NS produced a favorable systemic cytokine profile for tumoricidal activity within the peripheral blood. Whereas IFN-γ nadir occurred at 72 hours, levels recovered quickly and displayed positive correlations postburst out to 25 days postinjection. IL-12-NS administration induced proinflammatory changes while prompting minimal counterregulatory increases in anti-inflammatory IL-10 and IL-4 cytokine levels. Further, while IL-6 levels increased to 30 folds of the baseline during the burst phase, they normalized by 72 hours and trended negatively throughout the sill phase. Similar trends were observed with IL-1β and CXCL-1, suggesting a decreased likelihood of progression to a systemic inflammatory response syndrome-like state. As IL-12-NS delivers logarithmically lower amounts of IL-12 than previously administered during human clinical trials, our data reflect the importance of IL-12-NS which safely create a systemic immunostimulatory environment.

1. Introduction

Immunostimulation is a rapidly evolving concept in the field of immunooncology. While once a controversial topic, it is now well-established that intact immune systems can kill tumor cells [1]. The indiscriminate cytotoxicity of innate immunity combined with the antigen-specific cell surface receptor repertoire of adaptive immunity forms a highly effective network of host defense mechanisms that manage bodily insults of various etiologies, including tumorigenic cell transformation [2–4]. Currently, the most successful application of tumor immunotherapy has occurred using anticytotoxic T-lymphocyte-associated protein 4- (CTLA-4-) and/or antiprogrammed death-ligand 1- (PD-L1-) directed monoclonal antibodies as adjuvant treatment for lung and skin cancers [5]. However, checkpoint blockade alone has repeatedly failed to improve survival in other cancers including metastatic sarcoma over the current standard

of care [6], likely due to a combination of tumor-induced immunosuppressive forces that circumnavigate checkpoint blockade alongside extensive tumor cell pleomorphism [7]. Our group has shown that treatment modalities employing these "blocking the block" strategies can fail by prompting the emergence of tumor escape mechanisms [8].

Preclinical studies have shown that interleukin- (IL-) 12, an immunostimulatory cytokine, can induce strong antitumor responses against various malignancies. Compared to the monoclonal antibody checkpoint blockade, IL-12 is active over a broader spectrum of immune functions; examples of the effects of IL-12 include differentiation of T helper cells into the type one (T_H1) phenotype, stimulation of interferon-gamma production by macrophages, and enhanced cytotoxicity of natural killer (NK) cells [9, 10]. Preclinical studies have also shown that the antitumor effects of IL-12 are most pronounced when given systemically [11]. Unfortunately, clinical use of recombinant IL-12 systemically has been complicated by inadvertent overstimulation in the form of systemic inflammatory response syndrome (SIRS) and T cell exhaustion (TCE) [12], as high loading doses of free protein were needed to ensure adequate distribution to target tissues. Nevertheless, while the side-effect profiles of systemic high-dose IL-12 administration are toxic, low doses of IL-12 are generally safe [13]. If formulated correctly, recombinant IL-12 may be used to alter the local cytokine environment and encourage antitumor immunity at a point far enough upstream in the inflammatory cascade to induce a multimodal downstream response, ultimately leading to a decreased likelihood of treatment resistance. Therefore, low-dose immunostimulatory cytokines coupled with proper real-time patient monitoring to ensure immune safety may produce subtle yet clinically beneficial antitumor immune activity without unwanted overstimulation [14].

Poly(lactide-co-glycolic) acid (PLGA) drug delivery vectors are Food and Drug Administration (FDA) approved and can elute a wide variety of substances as the polymer coating breaks down into metabolic intermediates [15]. Drug solubility, bioavailability, and particle stability can be individually altered by the organic coating, allowing for large shifts in the pharmacokinetic and pharmacodynamic properties of the encapsulate [16]. The negatively charged surfaces of PLGA particles are repelled by the glycocalyx which, along with their smaller size, allows for increased deposition within the interstitial space where they can elute their contents undisturbed [17]. Furthermore, to be used in systemic settings (versus intratumoral injections), nanospheres must be able to achieve safe and effective travel through the microvasculature of an organism (with capillaries being approximately 4-9 μm in diameter) with minimal risk of forming emboli [18]. Encapsulating IL-12 within PLGA nanospheres is a potential strategy to achieve adequate biodistribution and tissue deposition of sensitive protein molecules without the need for toxic loading doses that resulted in the failure of clinical trials in the past [13]. While there have been several studies describing the synthesis of IL-12-loaded microspheres [19–35], to date, successful submicron encapsulation and elution of a structurally intact protein have not been well established. In this manuscript, we describe the synthesis and characterization of IL-12-loaded nanospheres (IL-12-NS), as well as the *in vivo* cytokinome profile produced when administered systemically.

2. Materials and Methods

2.1. Materials. Dichloromethane (DCM, #320269), Resomer RG 756 S (PLGA, #719927), NaCl (#7647-14-5), and poly(-vinyl alcohol) (PVA, #341584) were purchased from Sigma-Aldrich (St. Louis, MO). Albumin from bovine serum (BSA), FITC conjugate (BSA-FITC, #A23015), penicillin-streptomycin 10,000 U/mL (Pen-Strep, #15140122), and Alexa Fluor 647 carboxylic acid, tris(triethylammonium) salt (Alexa 647, #A33084) were purchased from Thermo Fisher Scientific (Waltham, MA). Recombinant mouse IL-12 (p70) (carrier free) (rmIL-12, #577008) and mouse IL-12 (p70) ELISA MAX deluxe ELISA kits (#433606) were purchased from BioLegend (San Diego, CA). Gibco Fetal Bovine Serum Qualified Heat Inactivated US Origin (HI-FBS, #MT35011CV) and Corning Cell Culture Buffers: Dulbecco's Phosphate-Buffered Salt Solution 1X (DPBS, #21031CV) were purchased from Fisher Scientific (Pittsburgh, PA). Female BALB/c mice (6-8 weeks of age) (#000651) were purchased from the Jackson Laboratory (Bar Harbor, ME).

2.2. Synthesis of Blank and Alexa 647-, BSA-FITC-, and rmIL-12-Loaded PLGA Nanospheres Using the Double Emulsion/Solvent Evaporation (DESE) Method with Microsphere Removal and Ultracentrifugation. To create the oil phase, 800 mg of Resomer RG 756 S PLGA was dissolved in 32 mL DCM at room temperature (RT) for two hours using a magnetic stir bar at 500 RPM. To create the aqueous phase (2% PVA) of the emulsion, 2400 mg PVA and 96 mg NaCl were dissolved in 120 mL deionized water and microwaved for 10-second bursts in a standard kitchen microwave on the high setting until clear, then cooled on ice. Next, the first emulsion was made by suspending the encapsulation substrate (Alexa 647 [5 mg], BSA-FITC [5 mg], or rmIL-12 [25 μg]) in 1200 μL DPBS and adding to the oil phase, which was promptly stirred at 17500 RPM for 6 minutes on ice using a tissue homogenizer. Blank particles were prepared similarly, however, with no encapsulate. The second emulsion was formed by slowly pouring the first emulsion into 120 mL of the 2% PVA salt solution while being emulsified with the tissue homogenizer at 17500 RPM and continuing for a total of 8 minutes. The resulting suspension was then stirred for 16 hours with a magnetic stir bar at 750 RPM to evaporate the organic solvent. Once the solvent was evaporated, the resulting solution was spun at 3500 RPM thrice; following each spin, supernatant was collected and placed on ice, with the resulting pellet being resuspended. The particles were then washed twice with deionized water via ultracentrifugation at 20000 RPM for 40 minutes at 4 degrees Celsius before flash-freezing in liquid nitrogen and storing short term at -20 degrees Celsius.

2.3. Nanosphere Morphology. The morphology of the nanospheres was determined via scanning electron microscopy (SEM) using a Hitachi S-4700 scanning electron microscope (Tarrytown, NY). Briefly, lyophilized samples were mounted on metal stubs with carbon tape and prepared for imaging with a gold-targeting Denton Desk V sputter and carbon coater (Moorestown, NJ), which applies a thin layer of gold to the biosample under an argon gas atmosphere. To test the stabilizing ability of the sugar additive trehalose during the lyophilization process, 1 mL of 50 mmol/mL trehalose was added to a 1 mL aliquot of blank nanoparticles suspended in deionized water for a final trehalose concentration of 25 mmol/mL prior to lyophilization and subsequent gold sputter/SEM imaging.

2.4. Nanosphere Characterization. Nanosphere count and size distribution were determined in duplicate using the Malvern Panalytical NanoSight NS300 (Malvern, UK) at RT in deionized water with dilution factors of 1:50 and 1:14 for unloaded and rmIL-12-loaded batches, respectively. Nanosphere zeta potentials were determined using the Malvern Panalytical Zetasizer Nano Z at RT in deionized water with dilution factor of 1:50 for both unloaded and loaded batches. Results included are the product of biological duplicates ($n = 2$).

2.5. Nanosphere BSA-FITC Encapsulation. Z-stack images of BSA-FITC-loaded PLGA nanospheres were created using the Zeiss 710 confocal microscope (Cambridge, UK).

2.6. Nanosphere rmIL-12 Elution Profile. 500 million particles/mL of IL-12-NS were prepared in a nanosphere release buffer (NRB, 10% HI-FBS and 100 units/mL Pen-Strep in DPBS). At specified time points, nanospheres were pelleted at $10000 \times g$ for 15 minutes, and an aliquot of supernatant was sampled. In between sampling times, suspensions were incubated at 37 degrees Celsius with continuous agitation (750 RPM) using a Benchmark Scientific MultiTherm Cool-Heat-Shake (Edison, NJ). Each aliquot was stored at 4 degrees Celsius for at least 24 hours to equilibrate with the release buffer before determining rmIL-12 concentration through ELISA. Results included are the product of biological duplicates ($n = 2$).

2.7. Estimation of Encapsulation Efficiency (EE). The amount of IL-12 encapsulated and released by the IL-12-NS was estimated by summing the protein concentrations measured by ELISA over time. This sum was multiplied by the particle concentration (PC) as determined by NanoSight and the total volume of synthesized particles (V); this value was then divided by the total mass of IL-12 added during synthesis (25 μg) as shown in the following equation:

$$EE = \frac{\left(\sum_{i=0}^{i=5} pgIL\text{-}12_i \right) * PC * V}{25\,\mu g}. \tag{1}$$

Results included are the product of $n = 2$ biological duplicates.

2.8. In Vivo Alexa 647-Loaded PLGA Nanosphere Substrate Biodistribution and Safety Study. Female BALB/c mice received 1 mg/kg intravenous (tail vein) or intraperitoneal (i.p.) injections of Alexa 647-loaded PLGA nanospheres suspended in sterile saline. The In Vivo Imaging System (IVIS® SpectrumCT In Vivo Imaging System, PerkinElmer, Waltham, MA) was used to monitor fluorescence intensity and biodistribution over a 30-minute interval, at which time animals were humanely euthanized by CO_2 asphyxiation and their femurs and lungs harvested for Z-stack confocal microscopy (Zeiss Violet Confocal, Jena, Germany).

2.9. In Vivo Administration of IL-12-Loaded PLGA Nanospheres and Cytokine Analysis. Thirty female BALB/c mice received retroorbital (r.o.) administration of 250 million IL-12-loaded nanospheres in 250 μL sterile saline. Groups of 3 mice were euthanized at the following time points: 5 minutes, 6 hours, 12 hours, 24 hours, 48 hours, 72 hours, 96 hours, 11 days, 18 days, and 25 days ($n = 3$). At each time point, blood was collected through cardiac puncture. Blood concentrations of interferon-gamma (IFN-γ), IL-10, IL-12p70, IL-1β, IL-2, IL-4, IL-5, IL-6, chemokine (C-X-C motif) ligand 1 (CXCL-1), and tumor necrosis factor-alpha (TNF-α) were analyzed using the Meso Scale Discovery (Rockville, MD) V-PLEX Proinflammatory Panel 1 Mouse Kit per manufacturer protocol. Treated animals were compared to pooled control animal samples using Student's t test with $\alpha = 0.05$.

3. Results

3.1. Nanosphere Synthesis, Morphology, and Characterization. Unloaded (blank), Alexa 647-, BSA-FITC-, and rmIL-12-loaded PLGA nanospheres (IL-12-NS) were successfully synthesized using the DESE method with ultracentrifugation as described. The morphology of both blank (Figures 1(a)–1(c)) and rmIL-12-loaded (Figures 2(b) and 2(c)) PLGA nanospheres was determined using scanning electron microscopy (SEM) to be spherical in shape with a mean particle diameter of 201.7 ± 6.7 nm and 138.1 ± 10.8 nm, respectively; the blank and rmIL-12-loaded PLGA nanosphere counts for each batch were determined to be $6.49 \times 10^9 \pm 6.19 \times 10^8$ particles/mL and $1.66 \times 10^9 \pm 4.45 \times 10^8$ particles/mL, respectively (Table 1). The introduction of 25 g rmIL-12 during particle synthesis resulted in a decrease in zeta potential magnitude from -21.3 ± 0.808 mV to -15.1 ± 1.249 mV (Table 1).

3.2. Nanosphere BSA-FITC Encapsulation and Z-Stack Imaging. To determine whether the synthesized nanospheres could indeed encapsulate protein and not merely adsorb it to the outer surface, 5 mg FITC-labeled BSA was loaded into the nanospheres; the resulting batch was imaged using confocal microscopy to visualize the internal structure. As shown in Figure 2(a), Z-stacking analysis confirmed that BSA was both adsorbed to the surface and incorporated within the polymeric shell.

3.3. IL-12-NS Elution Profile. 500 million particles/mL of IL-12-NS were eluted in NRB; aliquots taken daily were
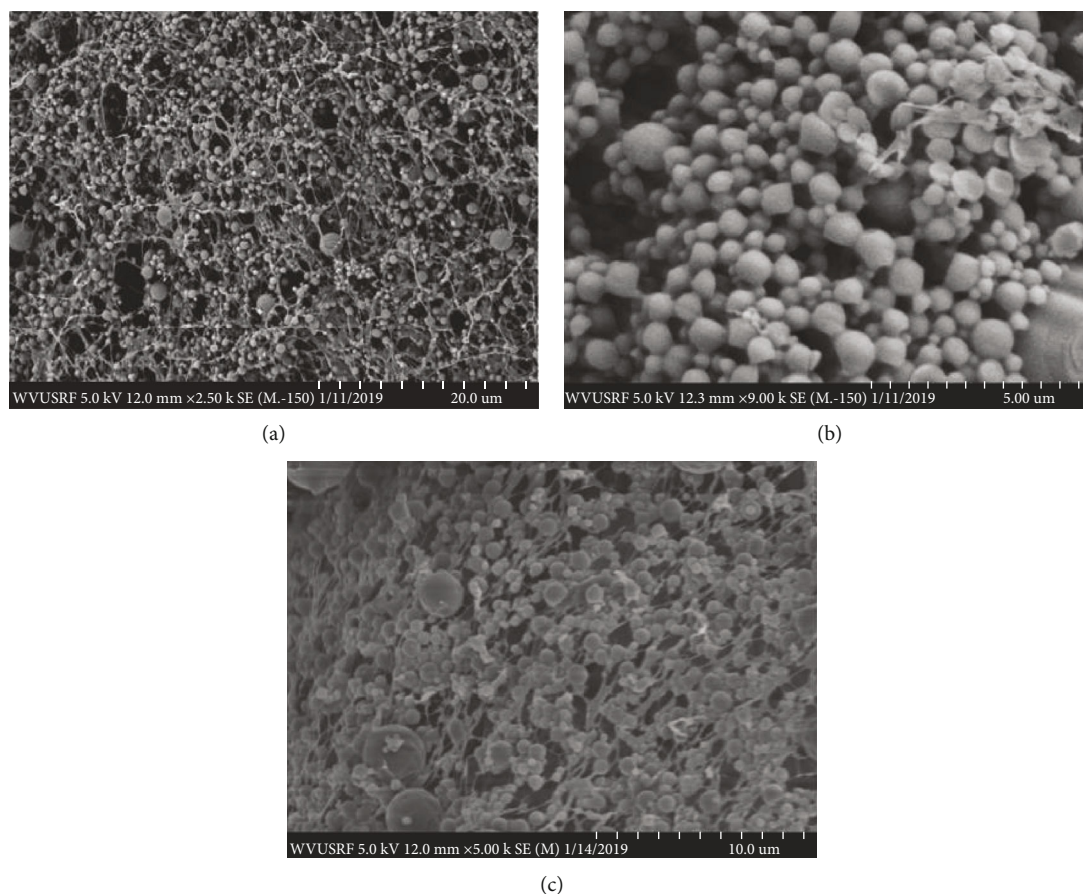
(a)

(b)

(c)

FIGURE 1: Scanning electron microscopy (SEM) images of unloaded (blank) poly(lactide-co-glycolic) acid (PLGA) nanospheres lyophilized without (a, b) and with (c) 25 mM trehalose at 2500x, 9000x, and 5000x magnifications, respectively.

subsequently analyzed with ELISA for heterodimeric p70 rmIL-12 concentrations released over time. The elution profiles for each particle concentration are shown in Figure 3, which displayed "burst" (days 0-1) and "sill" (days 1-5) phases characteristic of PLGA particle nanoencapsulation [36].

3.4. Estimation of Encapsulation Efficiency (EE). The amount of encapsulated rmIL-12 available for elution was estimated using Equation (1), and EE was determined to be 0.101 ± 0.009% (Table 1).

3.5. In Vivo Alexa 647-Loaded PLGA Nanosphere Substrate Biodistribution and Safety. We sought next to investigate whether the contents of PLGA nanospheres distribute systemically following injection without adverse events, including death. To accomplish this goal, PLGA nanospheres were loaded with Alexa 647 and administered to female BALB/c mice either intravenously (via tail vein) or intraperitoneally (i.p.) and monitored through IVIS imaging. At 30 minutes postinjection, both routes of administration resulted in systemic distribution of nanosphere contents (Figure 4(a)) without any signs of morbidity or mortality. Fluorescent microscopy following necropsy showed distribution of the encapsulate to both the lung and bone (Figure 4(b)).

3.6. In Vivo Characterization of Cytokinome Profile Induced by the Administration of IL-12-NS. We next evaluated the in vivo cytokinome profile induced by intravenous injection of 250 million IL-12-NS into BALB/c mice. This concentration was chosen because it was the highest particle count: saline ratio the mice could tolerate retroorbitally (data not shown). Following injection, groups of three [3] mice were euthanized at a total of ten [10] time points over the course of 25 days and blood cytokine concentrations were determined, normalized to control mice, and presented as the fold change from physiological baseline. For reference, a fold change of one (1) indicates equal cytokine levels in comparison to control, whereas a fold change of two (2) or one-half (0.5) indicates a respective doubling or halving from physiological levels. Although an oversimplification, for charting purposes, the cytokines were split into three groups by their generalized tumor-destroying (IFN-γ, IL-2, and IL-5), tumor-promoting (IL-10 and IL-4), or SIRS-associated (IL-1β, IL-6, CXCL-1, and TNF-α) properties [37–62].

3.6.1. Tumor-Destroying Cytokines: IFN-γ, IL-2, and IL-5. During the burst phase, blood concentrations of IFN-γ were significantly increased at 6 hours ($p < 0.05$) but significantly decreased at 12 hours ($p < 0.05$) (Figure 5(a)). During the sill phase, IFN-γ was also significantly decreased at 48 and 72
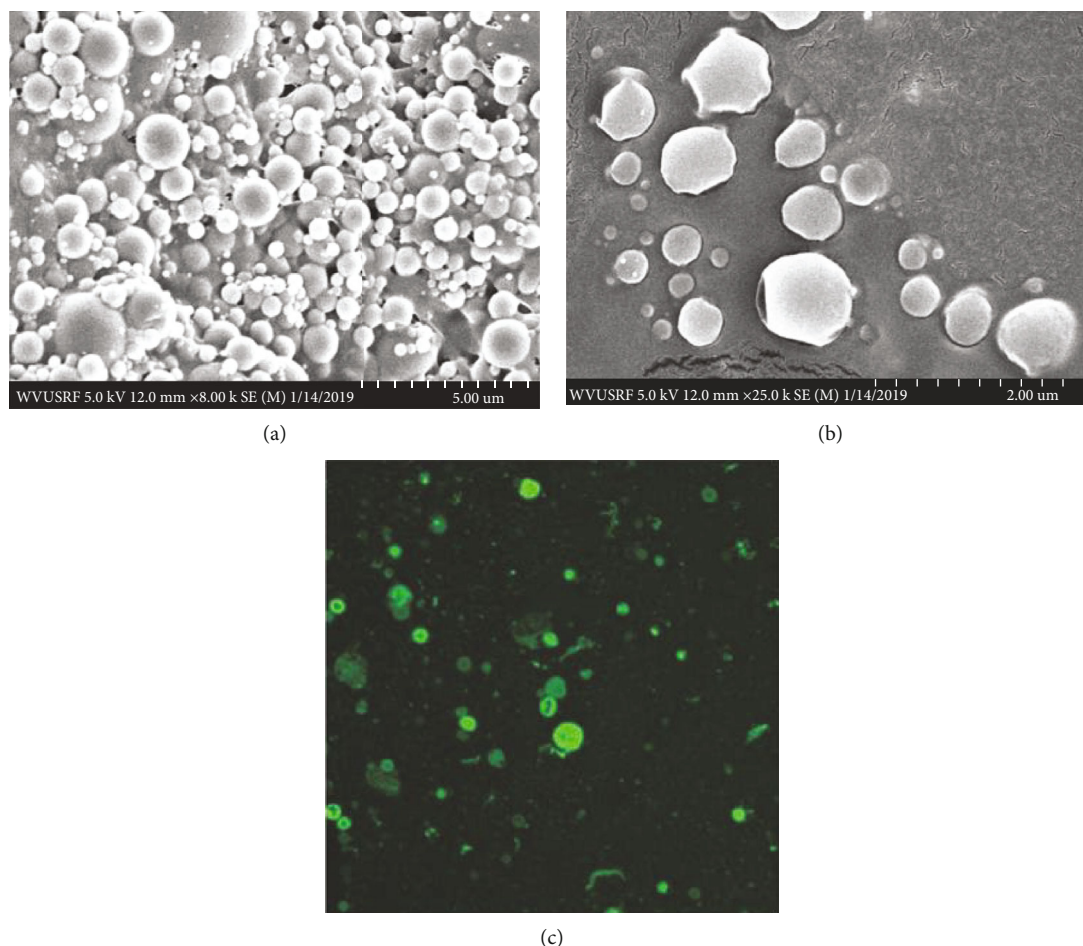
(a)

(b)

(c)

FIGURE 2: (a, b) Scanning electron microscopy (SEM) images of lyophilized recombinant mouse IL-12- (rmIL-12-) loaded PLGA nanospheres at 8000x and 25000x magnifications, respectively. (c) Fluorescein isothiocyanate- (FITC-) conjugated bovine serum albumin (BSA) was loaded into poly(lactide-co-glycolic) acid (PLGA) nanospheres, and the product was visualized for protein incorporation through confocal microscopy.

TABLE 1

	Average particle count (particles/mL)	Average ζ potential (mV)	Average EE (%)
Unloaded	$6.49 \times 10^9 \pm 6.19 \times 10^8$	-21.3 ± 0.808	N/A
Loaded	$1.66 \times 10^9 \pm 4.45 \times 10^8$	-15.1 ± 1.249	0.101 ± 0.009

EE: encapsulation efficiency (%).

hours ($p < 0.05$); however, it showed a positive trend across the sill phase ($R = 0.77$), with IFN-γ being elevated an average of 3.08-folds over the control at 25 days postinjection ($p = 0.052$, Figure 5(b)).

IL-2, albeit below physiologic levels, showed no significant fold changes during the burst phase (Figure 5(a)) but was significantly decreased at day 18 ($p < 0.05$) (Figure 5(b)). Further, it showed a positive trend across the sill phase; however, it did not return to baseline production levels during the 25-day sampling period ($R = 0.48$, Figure 5(b)).

Much like IL-2, IL-5 showed no significant fold changes during the burst phase (Figure 5(a)) but was significantly decreased at 24 hours postinjection ($p < 0.05$) (Figure 5(b)).

Similar to IFN-γ, IL-5 also showed a positive trend across the sill phase, exceeding physiological levels at both the 11- and 18-day time points postinjection although it was not statistically significant (Figure 5(b)).

3.6.2. Tumor-Promoting Cytokines: IL-10 and IL-4.
Tumor-promoting cytokines IL-10 and IL-4, though elevated in the 6-hour sample, showed no significant changes during the burst phase (Figure 5(c)). However, during the sill phase, IL-10 and IL-4 concentrations trended downward and remained near or below physiological levels after the 72- and 48-hour time points, respectively ($R = -0.51$ and -0.37, respectively, Figure 5(d)).

3.6.3. SIRS-Associated Cytokines: IL-1β, IL-6, CXCL-1, and TNF-α.
IL-1β was significantly increased at only the 6-hour time point ($p < 0.05$) throughout the 25-day sampling period postinjection during both the burst (Figure 5(e)) and sill phases (Figure 5(f)). It also showed a negative correlation across the sill phase, returning from those elevated levels to at or below physiological levels ($R = -0.54$, Figure 5(f)).
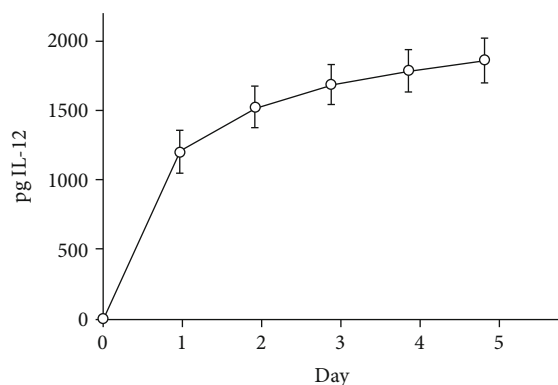
FIGURE 3: Cumulative amount of protein eluted over time from recombinant mouse IL-12-loaded poly(lactide-co-glycolic) acid (PLGA) nanospheres at a concentration of 500 million particles/mL as measured by ELISA. Nanospheres were eluted in $500\,\mu L$ of release buffer (NRB; 10% heat-inactivated fetal bovine serum [HI-FBS] and 100 units/mL Pen-Strep in DPBS) under constant agitation. Samples were collected from the supernatant following centrifugation of the pellet at $10000 \times g$ for 15 minutes at 4 degrees Celsius.

IL-6 was significantly elevated during the burst phase at 6- ($p < 0.01$) and 12- ($p < 0.001$) hour time points, reaching a transient maximum of a 30.58-fold increase over the control at 6 hours (Figure 5(e)). During the sill phase, IL-6 remained significantly increased at 24 hours ($p < 0.05$), 48 hours ($p < 0.01$), 96 hours ($p < 0.001$), and 18 days ($p < 0.05$) but, overall, trended downward ($R = -0.60$) and was statistically equivalent to the control by 25 days (Figure 5(f)).

During the burst phase, CXCL-1 was significantly elevated at 5 minutes ($p < 0.05$), 6 hours ($p < 0.001$), and 12 hours ($p < 0.05$). During the sill phase, it was significantly increased at 24 hours ($p < 0.01$) but displayed an overall negative correlation, returning to near baseline levels by the 72-hour time point ($R = -0.60$, Figure 5(f)).

TNF-α was significantly decreased during the burst phase at 5 minutes ($p < 0.05$) and 12 hours ($p < 0.001$) (Figure 5(e)). During the sill phase, TNF-α was significantly increased at 48 and 72 hours ($p < 0.05$) (Figure 5(f)). Interestingly, TNF-α was significantly decreased at 25 days ($p < 0.01$) (Figure 5(f)). Similar to the other SIRS-associated cytokines mentioned previously, TNF-α showed a negative correlation across the sill phase, returning to normal physiologic levels ($R = -0.46$, Figure 5(f)).

4. Discussion

Multiple cytokines have been shown to exhibit potent antitumor properties in preclinical studies; examples include IL-12, IL-2, IL-17, and IFN-γ among others [63]. IL-12, produced mainly by tumoricidal T_H1 cells, showed promise in animal models against a wide variety of tumor types including sarcoma, with best responses achieved through systemic versus local (intratumoral) administration [11]. Unfortunately, recombinant IL-12 cytokine therapy thus far has produced underwhelming results in human patients. Clinical trials conducted in the 1990s required high loading doses

of IL-12 to achieve adequate tissue biodistribution and resulted in TCE, SIRS, and ultimately worse outcomes [13]. In contrast, low-dose IL-12 given over prolonged periods has been shown to induce tumor regression without overstimulation, though there are currently few cases reported in the literature using this treatment strategy [64, 65]. Encapsulation in PLGA nanospheres may provide an opportunity to achieve slow and controlled delivery of IL-12 in a systemic fashion while ensuring delivery of contents to peripheral tissues.

IL-12-NS eluted picogram-scale protein doses corresponding to the equivalent of approximately 2-3.3 ng over the course of five days, and their diameter fell within a size distribution range of 100-200 nm. Notably, the zeta potential of loaded batches decreased in magnitude an average of 6.2 mV, which may reflect adsorption of rmIL-12 to the outer shell of the polymer coating [66]. The EE of our synthesis method was low (0.101%) and likely was due to the incorporation of rmIL-12 within microspheres, which comprises most of the formed product and is ultimately discarded during nanosphere purification. While other methods of synthesis (e.g., sonication) could have been employed for better encapsulation, bioactive IL-12 has a dimeric structure and is held together by a single disulfide bond that could easily be disrupted by vigorous agitation methods.

The *in vivo* studies provide a glimpse of the effects of IL-12-NS therapy on the systemic immune system. The biodistribution study suggested that the PLGA nanospheres (1) did not immediately flocculate and subsequently embolize and (2) distributed their contents systemically. As our group is primarily interested in metastatic osteosarcoma, we were especially excited to witness the distribution of nanosphere contents to the bone and lung. Further, V-PLEX analysis revealed significant changes in the cytokinome profiles of IL-12-NS-treated mice. Corresponding to the leukopenia observed in clinical trials following exogenous IL-12 administration, IFN-γ nadir occurred at 72 hours; however, in contrast to clinical trials, levels recovered quickly and displayed positive correlations postburst out to 25 days [67, 68]. The rapid recovery of secretory capacity following IL-12-NS administration suggests a lower likelihood of irreversible overstimulation.

Further, while serum IFN-γ levels in early clinical trials showed increasingly diminished responses to IL-12 over time, IL-12-NS-treated mice showed the opposite trend, which started at the onset of the sill phase and remained out to 25 days. Moreover, IL-12-NS administration induced these proinflammatory changes while prompting minimal counterregulatory increases in anti-inflammatory IL-10 and IL-4 cytokine levels [69, 70]. As SIRS is the most feared complication of recombinant cytokine therapy, IL-12-NS-induced increases in SIRS-associated cytokines could indicate dose-limiting toxicity. Although IL-6 levels increased to 30-folds of the baseline during the burst phase, they normalized by 72 hours and trended negatively throughout the sill phase. Similar trends were observed with IL-1β and CXCL-1, suggesting the potential for immune recovery and decreased likelihood of progression to a SIRS-like state. The increase of IFN-γ over time alongside the negative
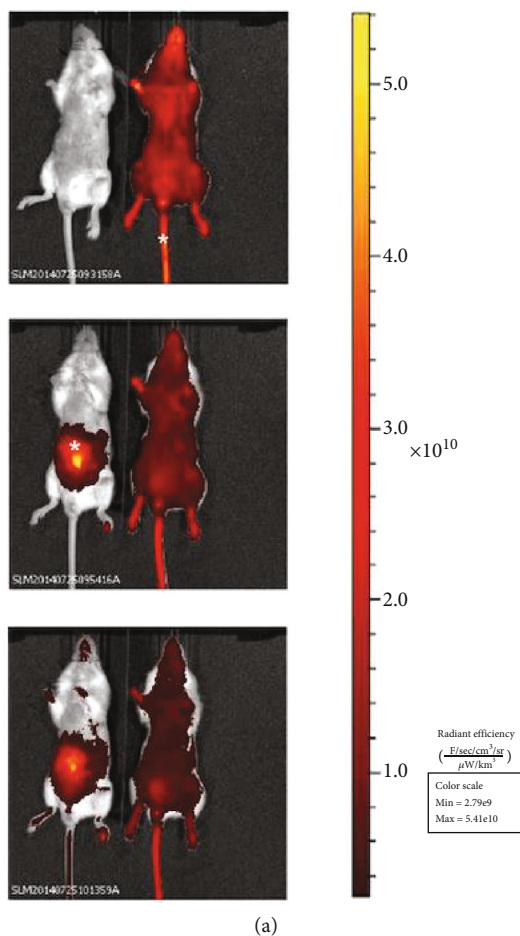
(a)
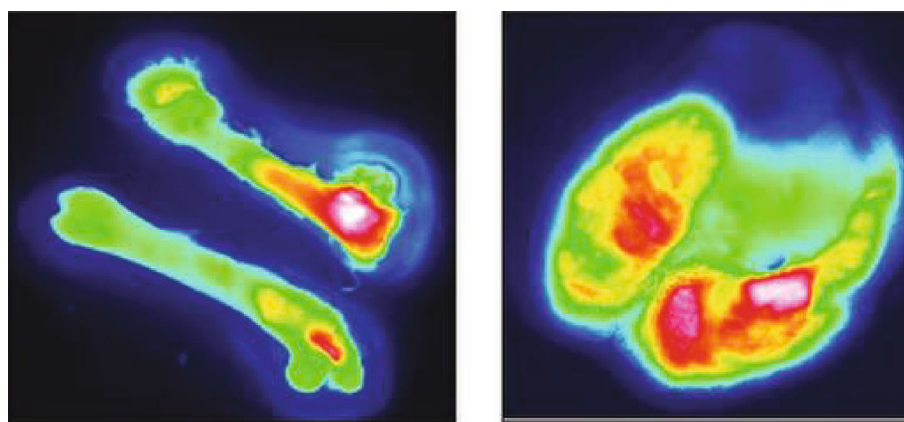
(b)

Figure 4: Female BALB/c mice were inoculated with 1 mg/kg of Alexa 647-loaded nanospheres dissolved in sterile saline and monitored for fluorophore distribution (a) systemically over 30 minutes (images presented by time from top [initial tail vein injection], middle [initial i.p. injection], to bottom [30 minutes postinjection]) via IVIS imaging through i.p. (left) and tail vein (right) injections (∗ indicates IVIS signal immediately following either injection) and (b) in the bone (left) and lung (right) at four hours postinjection via fluorescent microscopy.

correlate of IL-10 and little to no change in TNF-α as well as IL-6 suggests that repeated administration of low-dose IL-12 through the vector system IL-12-NS may not produce an exhaustive cytokinome believed to be associated with treatment failures in previous clinical trials [71]. Given the initial increase in IFN-γ with a sustained increase over several weeks in conjunction with a short increase in TNF-α that normalizes quickly (within 96 hours), and IL-10 levels that essentially never change, the cytokinome is set perfectly to achieve sustained immunostimulation without firing the immunosuppressive response. All of these positive responses are seen despite utilizing logarithmically lower doses than
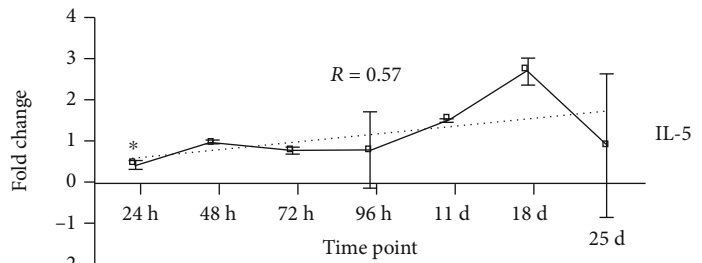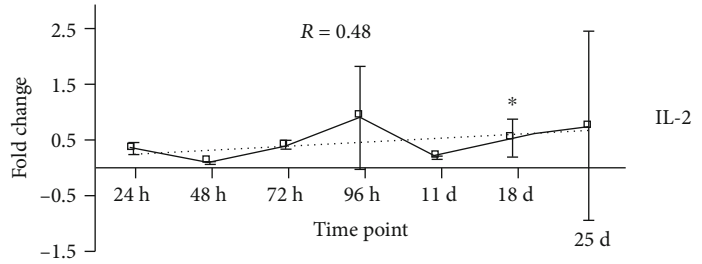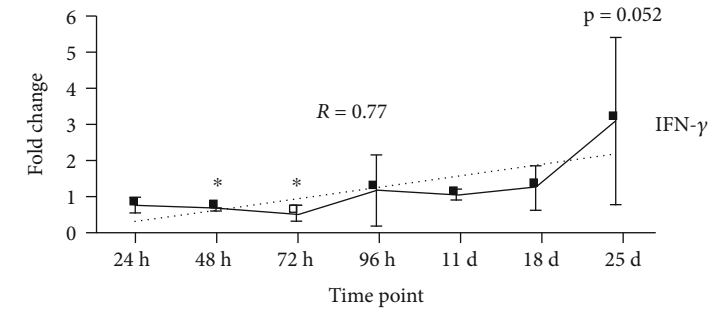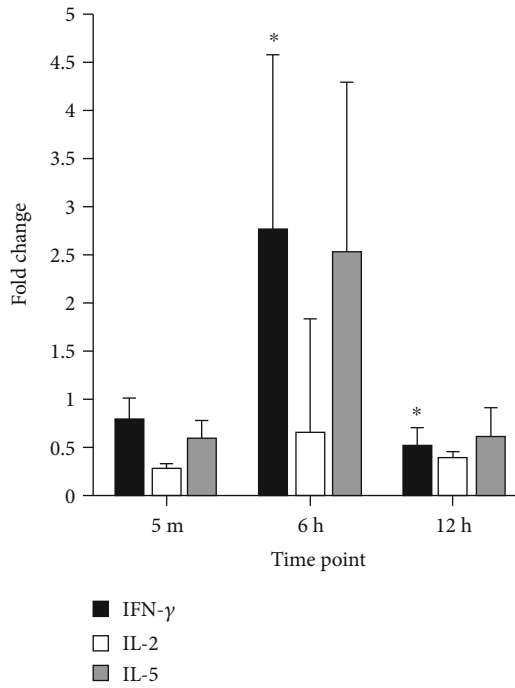
(a)
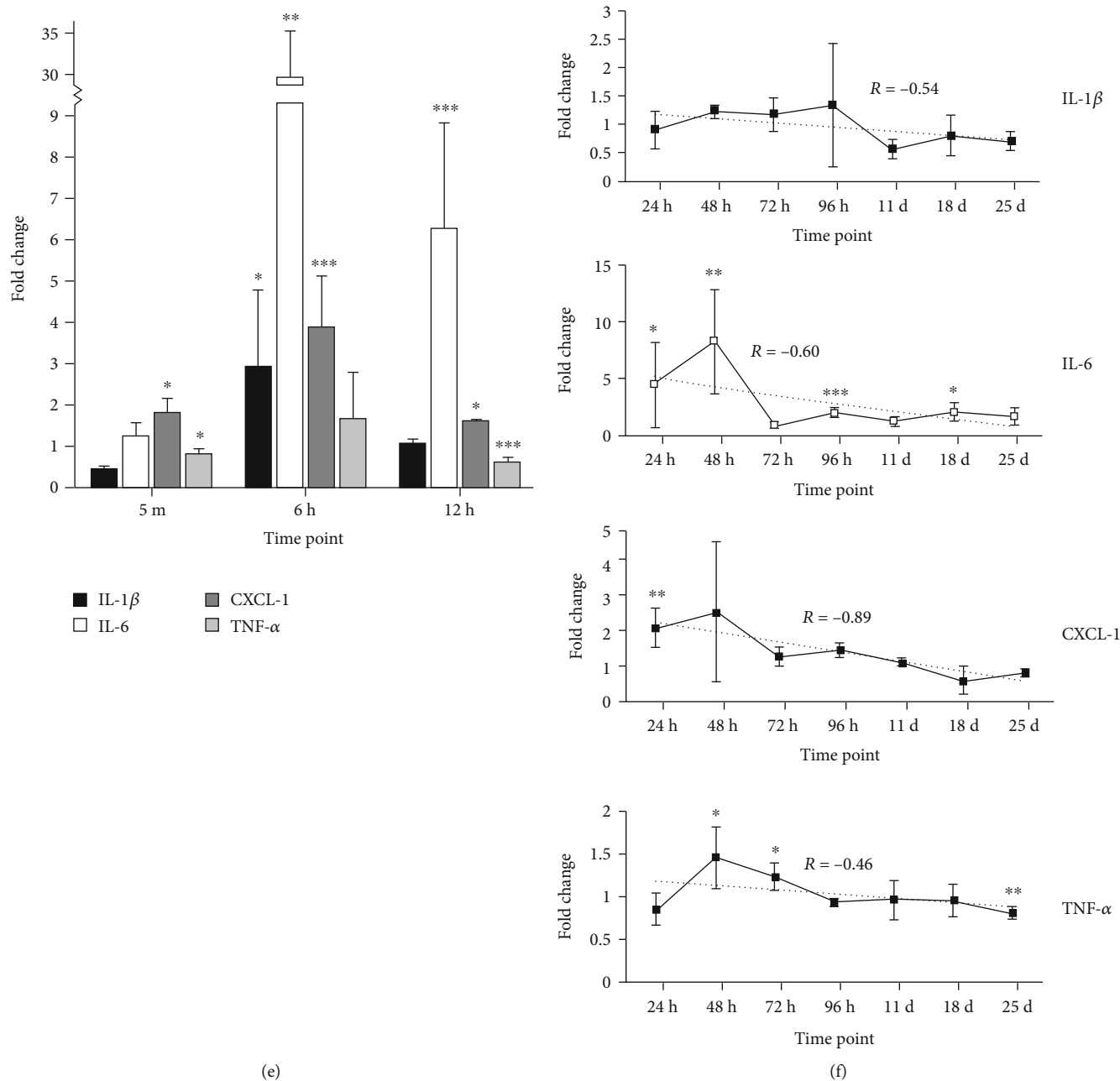
(b)
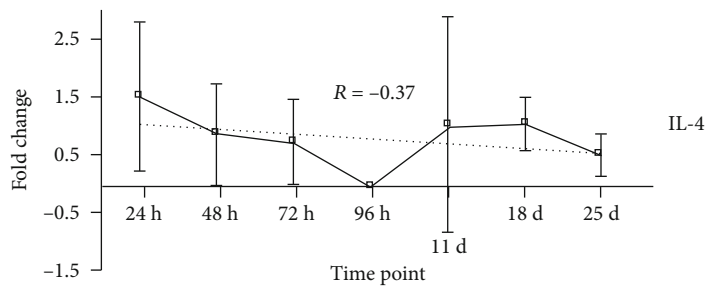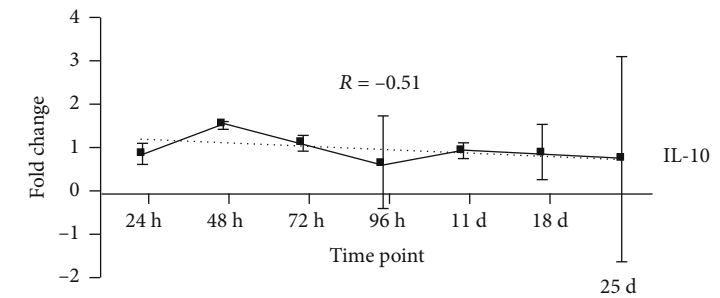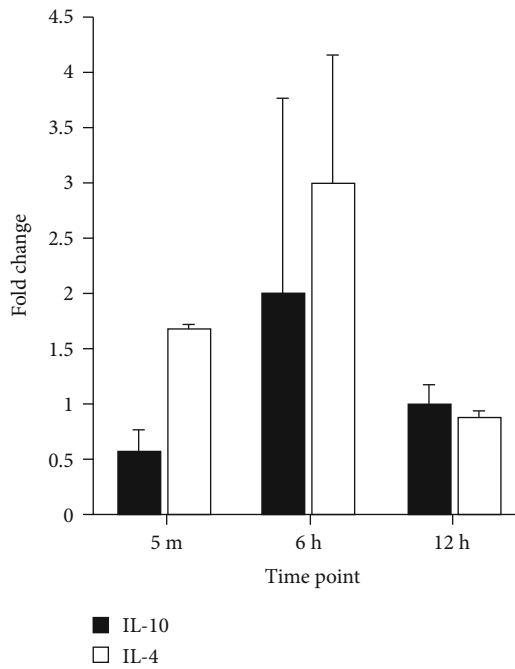
(c)

(d)

FIGURE 5: Continued.

(e)

(f)

FIGURE 5: Blood cytokine concentrations of $n = 3$ mice euthanized at various time points following retroorbital inoculation of 250 million recombinant mouse IL-12-loaded PLGA nanospheres. Samples normalized to six control mouse cytokinomes and represented as fold change. For reference, a fold change of one (1) indicates equal cytokine levels in comparison to control, whereas a fold change of two (2) or one-half (0.5) indicates a respective doubling or halving from physiological levels. Tumor-destroying cytokines, IFN-γ, IL-2, and IL-5, were sampled at (a) the burst phase—5 minutes (5 m), 6 hours (6 h), and 12 hours (12 h), and (b) the sill phase—24 hours (24 h), 48 hours (48 h), 72 hours (72 h), 96 hours (96 h), 11 days (11 d), 18 days (18 d), and 25 days (25 d), postinoculation. Tumor-promoting, IL-10, IL-4, and IL-5 (c, d), and SIRS-associated, IL-1β, IL-6, CXCL-1, and TNF-α (e, f), cytokines are also displayed at the same time points, graphically separated into burst and sill phases. Statistical differences were determined using Student's t test. $^*p < 0.05$, $^{**}p < 0.01$, and $^{***}p < 0.001$.

those delivered during human clinical trials (even when calculated as a ng/kg/day dosing assessment). These data further suggest the importance of the vector system which safely creates the antitumor, immunostimulatory environment sought by previous researchers.

5. Conclusion

From these results, we conclude that rmIL-12 can be effectively packaged into PLGA nanospheres using the double emulsion/solvent evaporation (w1/o/w2) technique with

ultracentrifugation and can achieve a homogenous distribution with a mean particle diameter of 138.1 ± 10.8 nm. Additionally, the nanospheres produced a characteristic elution profile with early "burst" and late steady-state "sill" phases with an average steady-state elution of 15 picograms IL-12/day at a starting concentration of 250 million spheres/mL. For the *in vivo* portion of the study, we found that IL-12-loaded nanospheres produced a systemic cytokine profile favoring immunostimulation without long-term elevation of SIRS-inducing acute phase response cytokines. While a larger experimental group may need to be tested to further validate our results, we suggest that IL-12-loaded nanospheres can produce antitumor immune profiles without inducing TCE and SIRS which is deserving of further investigation.

Data Availability

The datasets generated and/or analyzed in the current study are available from the corresponding author on reasonable request.

Disclosure

Conflicts of Interest

Dr. Brock A. Lindsey, MD, is founder of ICaPath Inc., which holds the worldwide exclusive license to the technology presented in this work from West Virginia University Research Corporation. No other authors declare any financial conflicts.

Authors' Contributions

Ryan A. Lacinski and Justin E. Markel are co-first authors.

Acknowledgments

References

[1] A. Finck, S. I. Gill, and C. H. June, "Cancer immunotherapy comes of age and looks for maturity," *Nature Communications*, vol. 11, no. 1, p. 3325, 2020.

[2] Y. Liu and G. Zeng, "Cancer and innate immune system interactions: translational potentials for cancer immunotherapy," *Journal of Immunotherapy*, vol. 35, no. 4, pp. 299–308, 2012.

[3] D. Pardoll, "Cancer and the immune system: basic concepts and targets for intervention," *Seminars in Oncology*, vol. 42, no. 4, pp. 523–538, 2015.

[4] N. Bhardwaj, "Harnessing the immune system to treat cancer," *The Journal of Clinical Investigation*, vol. 117, no. 5, pp. 1130–1136, 2007.

[5] L. Gu, P. A. Khadaroo, H. Su et al., "The safety and tolerability of combined immune checkpoint inhibitors (anti-PD-1/PD-L1 plus anti-CTLA-4): a systematic review and meta-analysis," *BMC Cancer*, vol. 19, no. 1, p. 559, 2019.

[6] V. Siozopoulou, A. Domen, K. Zwaenepoel et al., "Immune checkpoint inhibitory therapy in sarcomas: is there light at the end of the tunnel?," *Cancers (Basel)*, vol. 13, no. 2, p. 360, 2021.

[7] S. P. Kubli, T. Berger, D. V. Araujo, L. L. Siu, and T. W. Mak, "Beyond immune checkpoint blockade: emerging immunological strategies," *Nature Reviews. Drug Discovery*, vol. 20, no. 12, pp. 899–919, 2021.

[8] J. E. Markel, J. Noore, E. J. Emery, H. J. Bobnar, E. S. Kleinerman, and B. A. Lindsey, "Using the spleen as an in vivo systemic immune barometer alongside osteosarcoma disease progression and immunotherapy with α-PD-L1," *Sarcoma*, vol. 2018, Article ID 8694397, 13 pages, 2018.

[9] P. Scott, "IL-12: initiation cytokine for cell-mediated immunity," *Science*, vol. 260, no. 5107, pp. 496-497, 1993.

[10] W. T. Watford, M. Moriguchi, A. Morinobu, and J. J. O'Shea, "The biology of IL-12: coordinating innate and adaptive immune responses," *Cytokine & Growth Factor Reviews*, vol. 14, no. 5, pp. 361–368, 2003.

[11] F. Cavallo, E. Di Carlo, M. Butera et al., "Immune events associated with the cure of established tumors and spontaneous metastases by local and systemic interleukin 12," *Cancer Research*, vol. 59, no. 2, pp. 414–421, 1999.

[12] W. Lasek, R. Zagożdżon, and M. Jakobisiak, "Interleukin 12: still a promising candidate for tumor immunotherapy?," *Cancer Immunology, Immunotherapy*, vol. 63, no. 5, pp. 419–435, 2014.

[13] J. E. Markel, R. A. Lacinski, and B. A. Lindsey, "Nanocapsule delivery of IL-12," *Advances in Experimental Medicine and Biology*, vol. 1257, pp. 155–168, 2020.

[14] H. G. Pratt, E. M. Justin, and B. A. Lindsey, "Applying osteosarcoma immunology to understand disease progression and assess immunotherapeutic response," *Advances in Experimental Medicine and Biology*, vol. 1258, pp. 91–109, 2020.

[15] K. Avgoustakis, "Polylactic-co-glycolic acid (PLGA)," *Encyclopedia of Biomaterials and Biomedical Engineering*, vol. 1, no. 1, pp. 1–11, 2005.

[16] M. S. Muthu, "Nanoparticles based on PLGA and its co-polymer: an overview," *Asian Journal of Pharmaceutics (AJP)*, vol. 3, no. 4, 2009.

[17] R. A. Jain, "The manufacturing techniques of various drug loaded biodegradable poly(lactide-co-glycolide) (PLGA) devices," *Biomaterials*, vol. 21, no. 23, pp. 2475–2490, 2000.

[18] W. W. Yang and E. Pierstorff, "Reservoir-based polymer drug delivery systems," *Journal of Laboratory Automation*, vol. 17, no. 1, pp. 50–58, 2012.

[19] N. K. Egilmez, Y. S. Jong, M. S. Sabel, J. S. Jacob, E. Mathiowitz, and R. B. Bankert, "In situ tumor vaccination with interleukin-12-encapsulated biodegradable microspheres: induction of tumor regression and potent antitumor immunity," *Cancer Research*, vol. 60, no. 14, pp. 3832–3837, 2000.

[20] M. S. Sabel, J. Skitzki, L. Stoolman et al., "Intratumoral IL-12 and TNF-alpha-loaded microspheres lead to regression of breast cancer and systemic antitumor immunity," *Annals of Surgical Oncology*, vol. 11, no. 2, pp. 147–156, 2004.

[21] M. S. Sabel, A. Arora, G. Su, E. Mathiowitz, J. J. Reineke, and A. E. Chang, "Synergistic effect of intratumoral IL-12 and TNF-α microspheres: systemic anti-tumor immunity is mediated by both CD8+ CTL and NK cells," *Surgery*, vol. 142, no. 5, pp. 749–760, 2007.

[22] H. C. Hill, T. F. Conway, M. S. Sabel et al., "Cancer immunotherapy with interleukin 12 and granulocyte-macrophage colony-stimulating factor-encapsulated microspheres: coinduction of innate and adaptive antitumor immunity and cure of disseminated disease," *Cancer Research*, vol. 62, no. 24, pp. 7254–7263, 2002.

[23] A. U. Shah and M. J. D'Souza, "Sustained-release interleukin-12 microspheres in the treatment of cancer," *Drug Development and Industrial Pharmacy*, vol. 25, no. 9, pp. 995–1004, 1999.

[24] S. K. Watkins, N. K. Egilmez, J. Suttles, and R. D. Stout, "IL-12 rapidly alters the functional profile of tumor-associated and tumor-infiltrating macrophages in vitro and in vivo," *Journal of Immunology*, vol. 178, no. 3, pp. 1357–1362, 2007.

[25] M. O. Kilinc, K. S. Aulakh, R. E. Nair et al., "Reversing tumor immune suppression with intratumoral IL-12: activation of tumor-associated T effector/memory cells, induction of T suppressor apoptosis, and infiltration of CD8+ T effectors," *Journal of Immunology*, vol. 177, no. 10, pp. 6962–6973, 2006.

[26] S. J. Ha, S. H. Park, H. J. Kim et al., "Enhanced immunogenicity and protective efficacy with the use of interleukin-12-encapsulated microspheres plus AS01B in tuberculosis subunit vaccination," *Infection and Immunity*, vol. 74, no. 8, pp. 4954–4959, 2006.

[27] M. A. Kuriakose, F. A. Chen, N. K. Egilmez et al., "Interleukin-12 delivered by biodegradable microspheres promotes the antitumor activity of human peripheral blood lymphocytes in a human head and neck tumor xenograft/SCID mouse model," *Head & Neck*, vol. 22, no. 1, pp. 57–63, 2000.

[28] B. J. Han, J. D. Murphy, S. Qin et al., "Microspheres encapsulating immunotherapy agents target the tumor-draining lymph node in pancreatic ductal adenocarcinoma," *Immunological Investigations*, vol. 49, no. 7, pp. 808–823, 2020.

[29] D. A. Zaharoff, K. W. Hance, C. J. Rogers, J. Schlom, and J. W. Greiner, "Intratumoral immunotherapy of established solid tumors with chitosan/IL-12," *Journal of Immunotherapy*, vol. 33, no. 7, pp. 697–705, 2010.

[30] A. Arora, G. Su, E. Mathiowitz, J. Reineke, A. E. Chang, and M. S. Sabel, "Neoadjuvant intratumoral cytokine-loaded microspheres are superior to postoperative autologous cellular vaccines in generating systemic anti-tumor immunity," *Journal of Surgical Oncology*, vol. 94, no. 5, pp. 403–412, 2006.

[31] S. D. Hess, N. K. Egilmez, N. Bailey et al., "Human CD4+ T cells present within the microenvironment of human lung tumors are mobilized by the local and sustained release of IL-12 to kill tumors in situ by indirect effects of IFN-gamma," *Journal of Immunology*, vol. 170, no. 1, pp. 400–412, 2003.

[32] L. Broderick, S. J. Yokota, J. Reineke et al., "Human CD4+ effector memory T cells persisting in the microenvironment of lung cancer xenografts are activated by local delivery of IL-12 to proliferate, produce IFN-gamma, and eradicate tumor cells," *Journal of Immunology*, vol. 174, no. 2, pp. 898–906, 2005.

[33] R. E. Nair, Y. S. Jong, S. A. Jones, A. Sharma, E. Mathiowitz, and N. K. Egilmez, "IL-12 + GM-CSF microsphere therapy induces eradication of advanced spontaneous tumors in her-2/neu transgenic mice but fails to achieve long-term cure due to the inability to maintain effector T-cell activity," *Journal of Immunotherapy*, vol. 29, no. 1, pp. 10–20, 2006.

[34] N. K. Egilmez, "Cytokine-encapsulated biodegradable microspheres for immune therapy," *Immunological Investigations*, vol. 49, no. 7, pp. 824–839, 2020.

[35] M. L. Salem, W. E. Gillanders, A. N. Kadima et al., "Review: novel nonviral delivery approaches for interleukin-12 protein and gene systems: curbing toxicity and enhancing adjuvant activity," *Journal of Interferon & Cytokine Research*, vol. 26, no. 9, pp. 593–608, 2006.

[36] C. Rodrigues de Azevedo, M. von Stosch, M. S. Costa et al., "Modeling of the burst release from PLGA micro- and nano-particles as function of physicochemical parameters and formulation characteristics," *International Journal of Pharmaceutics*, vol. 532, no. 1, pp. 229–240, 2017.

[37] A. Poggi, A. M. Massaro, S. Negrini, P. Contini, and M. R. Zocchi, "Tumor-induced apoptosis of human IL-2-activated NK cells: role of natural cytotoxicity receptors," *Journal of Immunology*, vol. 174, no. 5, pp. 2653–2660, 2005.

[38] N. L. Vujanovic, S. Yasumura, H. Hirabayashi et al., "Antitumor activities of subsets of human IL-2-activated natural killer cells in solid tissues," *Journal of Immunology*, vol. 154, no. 1, pp. 281–289, 1995.

[39] L. Mortara, E. Balza, A. Bruno, A. Poggi, P. Orecchia, and B. Carnemolla, "Anti-cancer therapies employing IL-2 cytokine tumor targeting: contribution of innate, adaptive and immunosuppressive cells in the anti-tumor efficacy," *Frontiers in Immunology*, vol. 9, p. 2905, 2018.

[40] S. K. Doberstein, "Bempegaldesleukin (NKTR-214): a CD-122-biased IL-2 receptor agonist for cancer immunotherapy," *Expert Opinion on Biological Therapy*, vol. 19, no. 12, pp. 1223–1228, 2019.

[41] I. N. Buhtoiarov, H. Lum, G. Berke, D. M. Paulnock, P. M. Sondel, and A. L. Rakhmilevich, "CD40 ligation activates murine macrophages via an IFN-gamma-dependent mechanism resulting in tumor cell destruction in vitro," *Journal of Immunology*, vol. 174, no. 10, pp. 6013–6022, 2005.

[42] J. Riemensberger, A. Böhle, and S. Brandau, "IFN-gamma and IL-12 but not IL-10 are required for local tumour surveillance in a syngeneic model of orthotopic bladder cancer," *Clinical and Experimental Immunology*, vol. 127, no. 1, pp. 20–26, 2002.

[43] M. Kateh Shamshiri, M. R. Jaafari, and A. Badiee, "Preparation of liposomes containing IFN-gamma and their potentials in cancer immunotherapy: in vitro and in vivo studies in a colon cancer mouse model," *Life Sciences*, vol. 264, article 118605, 2021.

[44] L. Showalter, B. J. Czerniecki, and G. K. Koski, "Th1 cytokines in conjunction with pharmacological Akt inhibition potentiate apoptosis of breast cancer cells in vitro and suppress tumor growth in vivo," *Oncotarget*, vol. 11, no. 30, pp. 2873–2888, 2020.

[45] G. Ni, L. Zhang, X. Yang et al., "Targeting interleukin-10 signalling for cancer immunotherapy, a promising and complicated task," *Human Vaccines & Immunotherapeutics*, vol. 16, no. 10, pp. 2328–2332, 2020.

[46] L. Yang, Y. Dong, Y. Li et al., "IL-10 derived from M2 macrophage promotes cancer stemness via JAK1/STAT1/NF-κB/

Notch 1 pathway in non-small cell lung cancer," *International Journal of Cancer*, vol. 145, no. 4, pp. 1099–1110, 2019.

[47] J. M. Vahl, J. Friedrich, S. Mittler et al., "Interleukin-10-regulated tumour tolerance in non-small cell lung cancer," *British Journal of Cancer*, vol. 117, no. 11, pp. 1644–1655, 2017.

[48] M. Shibata, K. Gonda, T. Shimura, K. Sakurai, and S. Takenoshita, "SIRS, CARS and MARS in relationship to cancer cachexia and its clinical implications," *Annals of Cancer Research and Therapy*, vol. 26, no. 1, pp. 54–59, 2018.

[49] C. A. Dinarello, J. A. Gelfand, and S. M. Wolff, "Anticytokine strategies in the treatment of the systemic inflammatory response syndrome," *Journal of the American Medical Association*, vol. 269, no. 14, pp. 1829–1835, 1993.

[50] A. A. Dahaba, G. A. El-Awady, P. H. Rehak, W. A. Farag, and W. F. List, "Effect of hemofiltration on the elimination of procalcitonin, TNF alpha, IL-1 beta, and IL-6 in septic patients," *Anesthesiology-Philadelphia then Hagerstown*, vol. 93, no. 3; SUPP/2, article A443-A, 2000.

[51] S. Gando, T. Kameue, S. Nanzaki, and Y. Nakanishi, "Cytokines, soluble thrombomodulin and disseminated intravascular coagulation in patients with systemic inflammatory response syndrome," *Thrombosis Research*, vol. 80, no. 6, pp. 519–526, 1995.

[52] J. Ren and S. Wu, "A burning issue: do sepsis and systemic inflammatory response syndrome (SIRS) directly contribute to cardiac dysfunction?," *Frontiers in Bioscience*, vol. 11, no. 1, pp. 15–22, 2006.

[53] V. Gocheva, H. W. Wang, B. B. Gadea et al., "IL-4 induces cathepsin protease activity in tumor-associated macrophages to promote cancer growth and invasion," *Genes & Development*, vol. 24, no. 3, pp. 241–255, 2010.

[54] S. E. Ito, H. Shirota, Y. Kasahara, K. Saijo, and C. Ishioka, "IL-4 blockade alters the tumor microenvironment and augments the response to cancer immunotherapy in a mouse model," *Cancer Immunology, Immunotherapy*, vol. 66, no. 11, pp. 1485–1496, 2017.

[55] E. J. Lee, S. J. Lee, S. Kim et al., "Interleukin-5 enhances the migration and invasion of bladder cancer cells via ERK1/2-mediated MMP-9/NF-κB/AP-1 pathway: involvement of the p21WAF1 expression," *Cellular Signalling*, vol. 25, no. 10, pp. 2025–2038, 2013.

[56] S. Oda, H. Hirasawa, H. Shiga, K. Nakanishi, K. Matsuda, and M. Nakamua, "Sequential measurement of IL-6 blood levels in patients with systemic inflammatory response syndrome (SIRS)/sepsis," *Cytokine*, vol. 29, no. 4, pp. 169–175, 2005.

[57] P. V. Giannoudis, P. J. Harwood, P. Loughenbury, M. Van Griensven, C. Krettek, and H. C. Pape, "Correlation between IL-6 levels and the systemic inflammatory response score: can an IL-6 cutoff predict a SIRS state?," *The Journal of Trauma*, vol. 65, no. 3, pp. 646–652, 2008.

[58] R. Bhargava, C. J. Altmann, A. Andres-Hernando et al., "Acute lung injury and acute kidney injury are established by four hours in experimental sepsis and are improved with pre, but not post, sepsis administration of TNF-α antibodies," *PLoS One*, vol. 8, no. 11, article e79037, 2013.

[59] J. Grommes and O. Soehnlein, "Contribution of neutrophils to acute lung injury," *Molecular Medicine*, vol. 17, no. 3-4, pp. 293–307, 2011.

[60] N. Ahuja, A. Andres-Hernando, C. Altmann et al., "Circulating IL-6 mediates lung injury via CXCL1 production after acute kidney injury in mice," *American Journal of Physiology. Renal Physiology*, vol. 303, no. 6, pp. F864–F872, 2012.

[61] Y. Wang, J. Roller, J. E. Slotta et al., "Distinct patterns of leukocyte recruitment in the pulmonary microvasculature in response to local and systemic inflammation," *American Journal of Physiology. Lung Cellular and Molecular Physiology*, vol. 304, no. 4, pp. L298–L305, 2013.

[62] P. Dahiya, "Burns as a model of SIRS," *Frontiers in Bioscience*, vol. 14, pp. 4962–4967, 2009.

[63] F. Belardelli and M. Ferrantini, "Cytokines as a link between innate and adaptive antitumor immunity," *Trends in Immunology*, vol. 23, no. 4, pp. 201–208, 2002.

[64] R. Parihar, P. Nadella, A. Lewis et al., "A phase I study of interleukin 12 with trastuzumab in patients with human epidermal growth factor receptor-2-overexpressing malignancies: analysis of sustained interferon gamma production in a subset of patients," *Clinical Cancer Research*, vol. 10, no. 15, pp. 5027–5037, 2004.

[65] M. S. Gokhale, V. Vainstein, J. Tom et al., "Single low-dose rHuIL-12 safely triggers multilineage hematopoietic and immune-mediated effects," *Experimental Hematology & Oncology*, vol. 3, no. 1, p. 11, 2014.

[66] S. Patil, A. Sandberg, E. Heckert, W. Self, and S. Seal, "Protein adsorption and cellular uptake of cerium oxide nanoparticles as a function of zeta potential," *Biomaterials*, vol. 28, no. 31, pp. 4600–4607, 2007.

[67] M. J. Robertson, C. Cameron, M. B. Atkins et al., "Immunological effects of interleukin 12 administered by bolus intravenous injection to patients with cancer," *Clinical Cancer Research*, vol. 5, no. 1, pp. 9–16, 1999.

[68] J. E. Portielje, W. H. Kruit, A. J. Eerenberg et al., "Subcutaneous injection of interleukin 12 induces systemic inflammatory responses in humans: implications for the use of IL-12 as vaccine adjuvant," *Cancer Immunology, Immunotherapy*, vol. 54, no. 1, pp. 37–43, 2005.

[69] L. Meyaard, E. Hovenkamp, S. A. Otto, and F. Miedema, "IL-12-induced IL-10 production by human T cells as a negative feedback for IL-12-induced immune responses," *Journal of Immunology*, vol. 156, no. 8, pp. 2776–2782, 1996.

[70] F. W. McNab, J. Ewbank, A. Howes et al., "Type I IFN induces IL-10 production in an IL-27-independent manner and blocks responsiveness to IFN-γ for production of IL-12 and bacterial killing in Mycobacterium tuberculosis-infected macrophages," *Journal of Immunology*, vol. 193, no. 7, pp. 3600–3612, 2014.

[71] J. E. Portielje, C. H. Lamers, W. H. Kruit et al., "Repeated administrations of interleukin (IL)-12 are associated with persistently elevated plasma levels of IL-10 and declining IFN-gamma, tumor necrosis factor-alpha, IL-6, and IL-8 responses," *Clinical Cancer Research*, vol. 9, no. 1, pp. 76–83, 2003.